Nanoscience & Nanotechnology

Directly Grown Graphene Buffer Layers on Silicon Carbide Enable Remote Epitaxy of Gallium Nitride	69
Scalable Device Integration via III-V Epitaxy on Patterned 2D Materials	70
Revealing Metal Redox Pathways up to Ambient Pressure via in-situ Transmission Electron Microscopy	71
Atomic Lift-off of Epitaxial Membranes for Cooling-free Infrared Detection	72
Cross-correlated AFM and TERS Imaging of Janus Transition Metal Dichalcogenide Monolayers	73
Scalable, Defect-tolerant Spinodal Metamaterials with Tunable Mechanical Properties	74
Dynamic Mechanical Responses of Shell-based Spinodal Metamaterials	75
Atomic Layer Etching of Overlying Epitaxial Graphene on Graphene Buffer Layer for a Scalable Remote Epitaxy Template	76
Fluctuations in Superconducting Nanowires	77
Laser-induced Graphene Supercapacitors	78
Hydrogen Gas Detection with MoS2-based Chemical Sensing Platform	79
Signatures of Chiral Superconductivity in Rhombohedral Graphene	80
Domain-controlled Growth of Two-dimensional Tin Selenide	81
Molecular Probe Adsorption as a Technique to Elucidate Corona Phase Molecular Recognition (CoPhMoRe) through Structure Property Relationships	82
Optimizing Contact Resistance of GaN p-FET Devices for CMOS Applications	83
Optical Detection of Proximity Effect Between WSe2 and Multiferroic Helimagnet Nil2	84
On-site Growth of Perovskite Nanocrystal Arrays for Integrated Nanodevices	85
Probing Operational Degradation Mechanism on Cd-free Red and Blue QD-quantum dot LEDs	
Solid State Solar Energy Storage from Persistently Luminescent Solar Concentrators	87
Electrical Double Layer Force Enabled Wafer-scale Transfer of van der Waals Materials	88

Directly Grown Graphene Buffer Layers on Silicon Carbide Enable Remote Epitaxy of Gallium Nitride

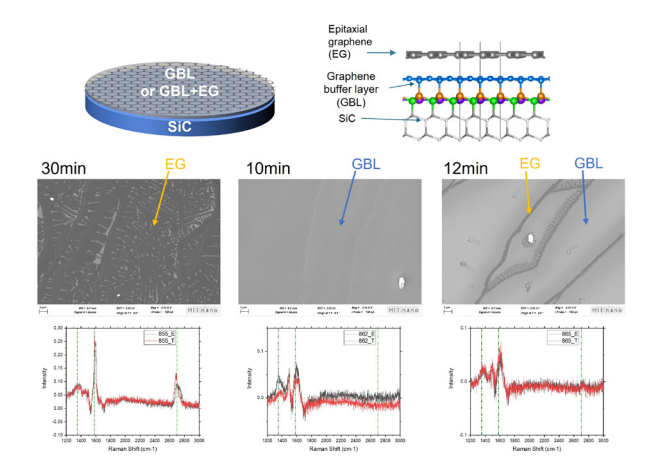
J. Kim, S. Lee, H. Kim, J. Kim, J. Lee, J. Feng, J. Kim Sponsorship: Samsung Display, Softepi

In the emerging technique of remote epitaxy, epitaxial films are grown on single-crystalline sub-strates coated with two-dimensional (2D) materials. Among these, graphene has been widely studied as a buffer layer and is typically transferred onto substrates via nickel-assisted delamination. However, this transfer process can damage the graphene, compromising the quality of the subsequent epitaxial film. To make matters worse, conventional epitaxial methods such as metal-organic chemical vapor deposition (MOCVD) present challenges, as reactive gases like H2 and NH3 can degrade graphene during high-temperature growth. To address this, we employ graphene buffer layers (GBLs) directly grown on silicon carbide (SiC), leveraging covalent bonding at the GBL-SiC interface while maintaining a van der Waals gap between GBL and the epitaxial films. This configuration enhances the stability of graphene under harsh growth conditions.

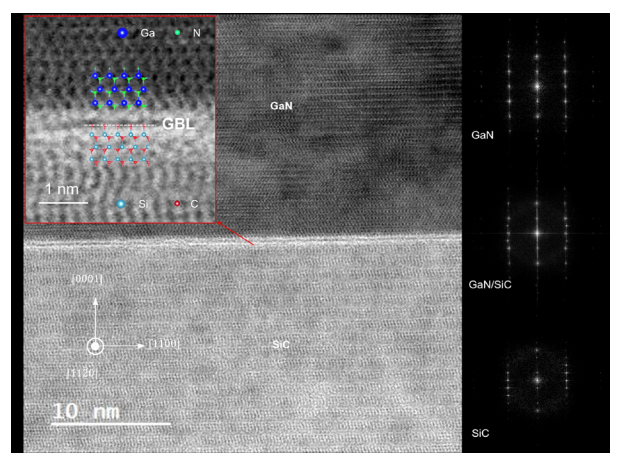
As Figure 1 shows, epitaxial graphene (EG) initially nucleates at step edges and subsequently extends

across terraces. Raman spectra, after subtraction of pristine SiC signals, exhibit the characteristic D (~1350 cm⁻¹), G (~1580 cm⁻¹), and 2D (~2700 cm⁻¹) peaks of graphene. The enhanced D peak and suppressed 2D peak confirm GBL formation. Based on these measurements, we identify the optimized growth conditions that suppress EG formation at step edges while enabling GBL growth on the substrate.

Subsequently, gallium nitride (GaN) is grown on GBL-coated SiC via MOCVD, as shown in Figure 2. Scanning transmission electron microscopy (STEM) confirms the preservation of the GBL after GaN growth, indicating its resilience under harsh MOCVD growth conditions. Corresponding fast Fourier transform (FFT) patterns indicate that GaN maintains a heteroepitaxial relationship with the SiC substrate, despite the presence of the GBL. These findings validate remote epitaxy, where the substrate's lattice information is transmitted through the graphene layer, enabling single-crystal GaN growth.



▲ Figure 1: Schematics of GBL and EG and their characterization by SEM and Raman. Fully covered EG shows strong 2D peaks; GBL-dominant regions exhibit stronger D peaks due to increased sp³ bonding.



▲ Figure 2: STEM cross section of GaN on SiC and corresponding FFT of GaN, GaN/SiC, and SiC. GBL remains after growth, confirming its stability. Diffraction confirms single-crystal GaN via remote epitaxy.

FURTHER READING

- S. Lee, J. Kim, B.-I. Park, H. Ik Kim, C. Lim, E. Lee, J. Y. Yang, J. Choi, et al. "GaN Remote Epitaxy on a Pristine Graphene Buffer Layer via Controlled Graphitization of SiC", Applied Physics Letts., vol. 125, p. 25, 2024.
- K. Qiao, Y. Liu, C. Kim, R. J. Molnar, T. Osadchy, W. Li, X. Sun, H. Li, et al. "Graphene Buffer Layer on SiC as a Release Layer for High-quality Free-standing Semiconductor Membranes," *Nano Letts.*, vol. 21, no. 9, pp. 4013-4020, 2021.
- Y. Kim, S. S. Cruz, K. Lee, B. O. Alawode, C. Choi, Y. Song, J. M. Johnson, C. Heidelberger, et al. "Remote Epitaxy Through Graphene Enables Two-dimensional Material-based Layer Transfer," *Nature*, vol. 544, no. 7650, pp. 340-343, 2017.

Scalable Device Integration via III-V Epitaxy on Patterned 2D Materials

N. M. Han, K. Lu, D. Kwon, C. Chang, J. Kim Sponsorship: Defense Advanced Research Projects Agency

The integration of high-mobility III-V semiconductors on scalable platforms is a critical step toward advancing future generations of high-performance electronic and optoelectronic devices. However, conventional III-V/Si heteroepitaxy faces severe challenges due to lattice and polarity mismatch, leading to high densities of threading dislocations and antiphase boundaries that degrade device performance. Existing approaches such as graded buffer layers and aspect ratio trapping have achieved partial success but still suffer from thick buffers, residual defects, and limited scalability.

Our research explores a novel integration strategy based on selective-area epitaxy of III-V materials on patterned two-dimensional (2D) materials. 2D materials like graphene serve as atomically thin, flexible buffer layers that mediate the lattice mismatch and allow lateral strain relaxation without generating dislocations. By engineering nanometer-scale openings (nanoholes) in the 2D layer, we localize III-V nucleation on the underlying substrate while suppressing unwanted nucleation elsewhere, enabling selective and defect-minimized epitaxy.

As a first step, we have demonstrated successful deoxidation of silicon substrates beneath nanoholes, enabling the nucleation of relaxed and dislocation-free GaAs crystals directly on silicon, as verified by high-resolution transmission electron microscopy. Furthermore, we have achieved a lateral-to-vertical growth rate ratio of approximately 20×, allowing efficient lateral overgrowth without significantly

increasing the vertical thickness. This high lateral growth rate is critical for eventual coalescence of adjacent III-V nuclei without the need for thick layers, offering a pathway toward ultrathin device channels.

Looking ahead, our next milestones include achieving full merging of III-V nuclei, characterizing the presence and nature of any defects at the coalescence boundaries, and fabricating and testing devices to benchmark electrical performance. While ${\rm SiO}_2$ trench confinement has been proposed to further control nucleation density and merging, it has not yet been implemented in the current stage of the work.

Ultimately, our approach aims to enable monolithic, transfer-free integration of III-V materials onto complementary metal-oxide-semiconductor-compatible platforms with minimal defects and atomically sharp heterojunctions. By circumventing the limitations of traditional heteroepitaxy, this technique could significantly advance the development of high-mobility transistors, such as III-V multiquantum well metal-oxide semiconductor field-effect transistors and gate-all-around structures, as well as low-defect optoelectronic devices.

Our preliminary success in demonstrating dislocation-free nucleation and efficient lateral overgrowth represents a major step toward scalable heterogeneous integration using 2D material-assisted epi-taxy. This platform holds promise for revolutionizing device scaling strategies and extending Moore's Law into new frontiers.

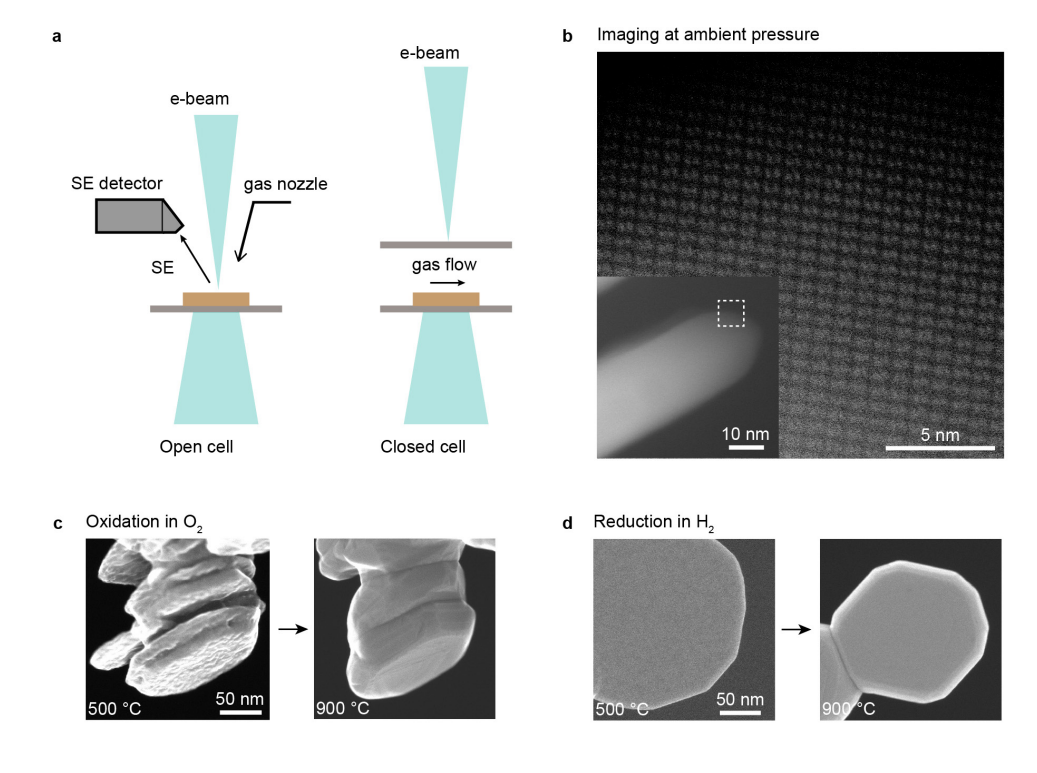
Revealing Metal Redox Pathways up to Ambient Pressure via in-situ Transmission Electron Microscopy

H. Wu, F. M. Ross

Sponsorship: Center for Electrification and Decarbonization of Industry, Seagate

Metal redox reactions are ubiquitous in nature (e.g., geological processes) and industrial applications. Understanding how materials evolve in morphology and structure at the nanoscale during such reactions in gaseous environments is critical for advancing catalysis, energy storage, and semiconductor technologies. Advances in transmission electron microscopy (TEM), microfabrication, and microelectromechanical systems have enabled the direct exposure of samples to a controlled gas environment at elevated temperatures within the microscope column. Gas can be introduced at low pressures (up to tens of millibars) using differential pumping or confined between two thin silicon nitride membranes in a closed-cell specimen holder (up to ambient pressure). Both approaches have proven effective in revealing atomistic mechanisms governing metal redox reactions. However, the effects of gas pressure on kinetic phase transformation pathways, particularly on transient surface morphological evolution during redox reactions, remain poorly understood.

In this project, we investigate metal redox reactions in various gaseous environments across different pressures using Characterization.nano's Hitachi HF5000-IS environmental TEM (ETEM) with a secondary electron (SE) detector (Figure 1). We visualize redox reactions occurring in a range of metal and alloys (Fe-, Zn-, and Ni-based alloys) under gases, including H2, O2, methanol, and water vapor, up to ambient pressure. These experiments demonstrate that atomic resolution can be obtained under ambient pressure conditions and enable us to identify several transient phase transformation pathways during the early stages of oxidation and reduction of metals. The simultaneous SE imaging enabled us to understand the surface morphological changes taking place during these reactions, including the removal of surface ligand layers and the development of surface faceting. We anticipate these advances will broaden the application of in-situ gas phase TEM for studying dynamic material processes.



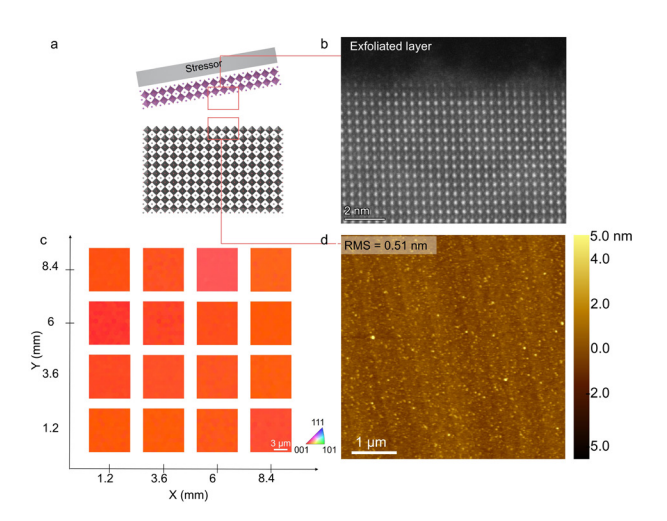
 \triangle Figure 1: (a) Schematics of setups for gas-phase TEM imaging. (b) Atomic-resolution image of magnetite in O_2 at am-bient pressure. (c-d) Secondary electron images showing the morphological evolution of magnetite oxidation in O_2 (c) and hematite reduction in H_2 (d).

Atomic Lift-off of Epitaxial Membranes for Cooling-free Infrared Detection

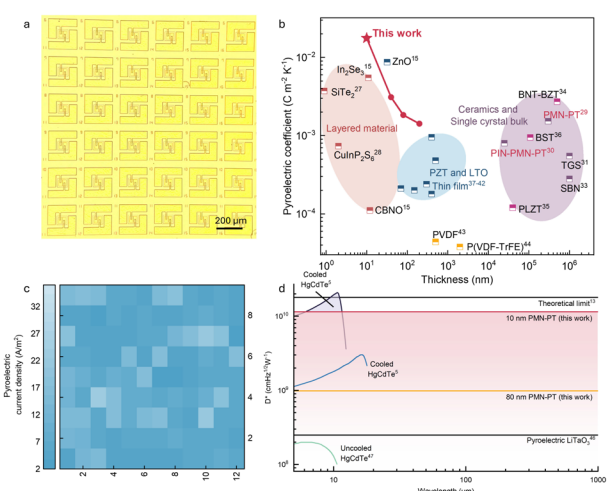
X. Zhang, O. Ericksen, S. Lee, M. Akl, M-K. Song, H. Lan, P. Pal, J. M. Suh, S. Lindemann, J-E. Ryu, Y. Shao, X. Zheng, N. M. Han, B. Bhatia, H. Kim, H. S. Kum, C. S. Chang, Y. Shi, C.-B. Eom, J. Kim Sponsorship: Air Force Office of the Scientific Research

Recent breakthroughs in ultrathin, single-crystalline, freestanding complex oxide systems have sparked industry interest in their potential for next-generation commercial devices. However, the mass production of these ultrathin complex oxide membranes has been hindered by the challenging requirement of inserting an artificial release layer between the epilayers and substrates. Here we introduce a technique that achieves atomic precision lift-off of ultrathin membranes without artificial release layers to facilitate the high-throughput production of scalable, ultrathin, freestanding perovskite systems (Figure 1). Leveraging both theoretical insights and empirical evidence, we

have identified the pivotal role of lead in weakening the interface. This insight has led to the creation of a universal exfoliation strategy that enables the production of diverse ultrathin perovskite membranes less than 10 nm thick. Our pyroelectric membranes demonstrate a record-high pyroelectric coefficient of 1.76×10^{-2} C m⁻² K⁻¹, attributed to their exceptionally low thickness and freestanding nature (Figure 2). Moreover, this method offers an approach to manufacturing cooling-free detectors that can cover the full far-infrared (FIR) spectrum, marking a notable advancement in detector technology.



▲ Figure 1: Atomic lift-off (ALO) of epitaxial ultrathin membranes at a large scale. (a) Schematic of ALO process. (b) Cross-section transmission electron microscopy image of exfoliated membrane. (c) Electron backscatter diffraction maps over the entire membrane. (d) Atomic-force microscopy image of substrate after exfoliation.



▲ Figure 2: Potential application towards cooling-free FIR imaging. (a) Optical image of pyroelectric device array fabricated on $Pb(Mg_{1/3}Nb_{2/3})O_3-PbTiO_3$ membrane. (b) Benchmark plot showing pyroelectric coefficients. (c) Mapping of the performance of device array. (d) Specific detectivity evaluations as a function of wavelength for our detector vs. commercial ones.

FURTHER READING

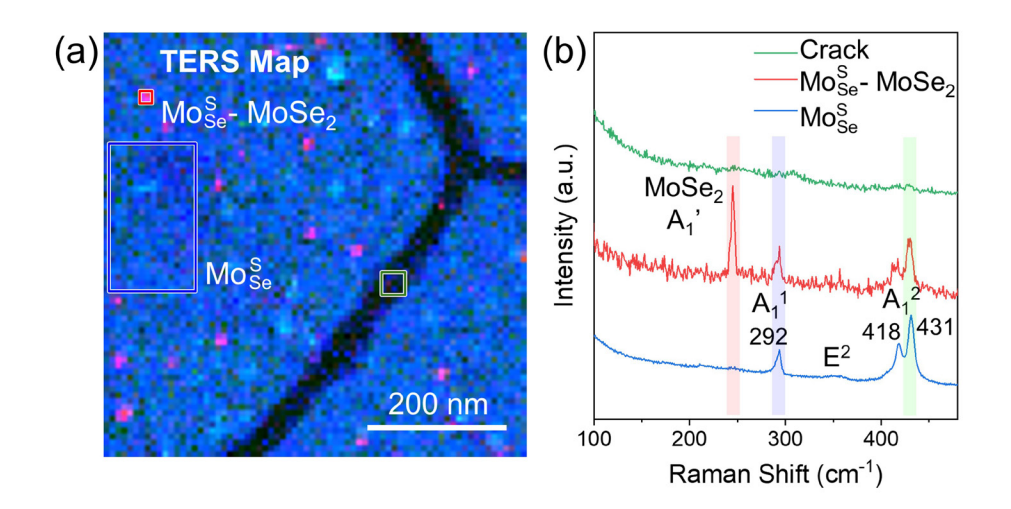
 X. Zhang, O. Ericksen, S. Lee, M. Akl, and J. Kim, "Atomic Lift-Off of Epitaxial Membranes for Cooling-Free Infrared Detection," Nature, vol. 641, pp. 98-105, May 2025.

Cross-correlated AFM and TERS Imaging of Janus Transition Metal Dichalcogenide Monolayers

T. Zhang, A. Krayev, T. H. Yang, N. Mao, L. Hoang, Z. Wang, H. Liu, Y. R. Peng, A. Mannix, J. Kong Sponsorship: U.S. Department of Energy, Office of Science, Basic Energy Sciences under Award DE-SC0020042.

Two-dimensional (2D) Janus transition metal dichalcogenides (TMDs) are intriguing material candidates for various applications such as non-linear optics, energy harvesting, and catalysis. These materials are usually synthesized via chemical conversion of pristine TMDs, and reliable and high-resolution characterization of the obtained Janus materials' morphology and composition is highly desired for both the synthesis optimization and device applications. In this work, we present a cross-correlated atomic force microscopy (AFM) and tip-enhanced Raman spectroscopy (TERS) study of Janus and Janus monolayers synthesized by the hydrogen plasma-assisted chemical conversion of MoSe₂ and MoS₂, respectively. Effects of strain and substrates

during the Janus conversion process on the morphology of resulting Janus TMD materials are revealed. Moreover, the TERS characterization shows nanoscale MoSe₂-Janus vertical heterostructures (~20-nm sizes) that become hidden under conventional far-field optical characterization, suggesting the power of using near-field approaches to avoid misconceptions in the composition of Janus TMDs. Our work indicates that cross-correlated AFM and TERS have great capability for studying nanoscale composition and defects in Janus TMD monolayers. The obtained insights into morphology and composition should be useful for further optimizing the Janus conversion approach towards uniform and wrinkle-/crack-free Janus materials.



▲ Figure 1: (a) TERS map showing intensity distribution of correspondingly highlighted Raman modes in panel (b): $MoSe_2A_1$ (red), A_1^2 (green), and $A1^1$ (blue). Map clearly identifies Janus monolayer (blue rectangle), nanoscale $MoSe_2$ -Janus vertical heterostructures (red square), and crack (green square) regions. (b) TERS spectra averaged over Janus monolayer , nanoscale $MoSe_2$ -Janus vertical heterostructures, and crack regions marked in (a).

FURTHER READING

[•] T. Zhang, A. Krayev, T. H. Yang, N. Mao, L. Hoang, Z. Wang, H. Liu, Y. R. Peng, et al., "Synthesis-related Nanoscale Defects in Mo-based Janus Monolayers Revealed by Cross-correlated AFM and TERS Imaging," arXiv:2503.22861 [cond-mat.mtrl-sci].

Scalable, Defect-tolerant Spinodal Metamaterials with Tunable Mechanical Properties

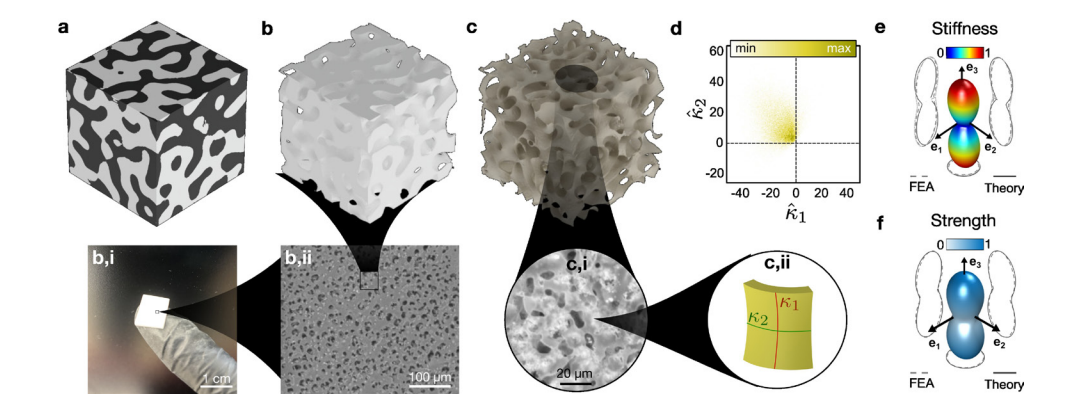
S. Dhulipala, M. A. Espinal, C. M. Portela Sponsorship: NSF CAREER

Spinodal metamaterials, non-periodic, bicontinuous structures inspired by nature, offer a scalable pathway to fabricating lightweight, high-performance materials with exceptional mechanical properties. Unlike truss-based lattices, which concentrate stress and rely on geometric periodicity, spinodal architectures eliminate sharp junctions and distribute stress smoothly through doubly curved shells. These features, combined with their compatibility with self-assembly and coating-based synthesis, open avenues for scale-bridging fabrication.

This work presents scalable strategies for generating spinodal geometries. We induce spinodal decomposition in epoxy-based polymer systems to produce large-scale templates with smooth, interconnected channels. Conformal nanocoating of these templates using ceramic thin films such as alumina followed by removal of the polymer template produces hollow, shell-based spinodal metamaterials with controlled wall thickness and curvature. Additionally, these templates are digitally

reconstructed using micro-scale X-ray computed tomography (XCT), enabling both structural characterization and theoretical modeling. To quantify how geometry affects performance, we introduce new curvature-based metrics for predicting anisotropic stiffness and strength. Local curvature distributions, derived from principal curvature maps, strongly correlate with measured and simulated mechanical response. These predictions are validated through two-photon lithography prototypes tested under in-situ nanomechanical compression, as well as finite element simulations. Our approach enables rational design and optimization of spinodal structures by controlling curvature anisotropy to tune mechanical properties.

With this scalable fabrication platform and new geometric framework, spinodal meta-materials emerge as a versatile solution for next-generation lightweight structures, overcoming the limitations of periodic lattices in defect tolerance, scalability, and mechanical tunability.



▲ Figure 1: Overview of scalable spinodal metamaterials. (a) Three-dimensional (3D) rendering of the spinodal decomposition process. (b) Epoxy template derived from spinodal decomposition, including (b,i) a large-scale fabricated template and (b,ii) scanning electron microscopy (SEM) image showing its bicontinuous morphology. (c) 3D rendering of a shell-based spinodal metamaterial, with (c,i) SEM image of an alumina spinodal shell structure and (c,ii) schematic illustrating the principal curvature directions on a representative shell element. (d) Distribution of principal curvature in the shell-based spinodal geometry. Theoretically predicted anisotropic (e) stiffness and (f) strength, derived from curvature-based geometric metrics.

FURTHER READING

C. M. Portela, A. Vidyasagar, S. Krödel, T. Weissenbach, D. W. Yee, J. R. Greer, and D. M. Kochmann, "Extreme Mechanical Resilience of Self-assembled Nanolabyrinthine Materials," Proc. Natl. Acad. Sci. U.S.A., vol. 117, no. 11, pp. 5686-5693, 2020. DOI.org/10.1073/pnas.1916817117

[•] S. Dhulipala, and C. M. Portela, "Curvature-Guided Mechanics and Design of Spinodal and Shell-Based Architected Materials," arXiv preprint arXiv:2505.21509, 2025. [Link]

Dynamic Mechanical Responses of Shell-based Spinodal Metamaterials

R. T. Kommalapati, C. M. Portela

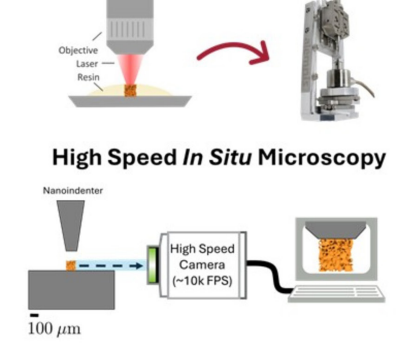
Architected materials are engineered materials that realize unique properties like near-optimal stiffness, strength, and energy absorption, mitigating vibrations or even focusing and guiding waves. There is high demand for lightweight materials with high energy absorption in many applications such as energy-absorbing bumpers, lightweight protective cladding, or shock-resistant medical impacts. Traditionally, architected materials have required high-resolution additive manufacturing to construct their carefully designed microstructure, a time- and cost-intensive process that can introduce significant performance-degrading defects. One area of recent interest has been spinodal metamaterials, which are the result of a natural phase separation process, granting a potential path to defect-free, inexpensive, and scalable fabrication. The resulting structures are aperiodic and asymmetric, consisting of smoothly connected shells with double curvature, analogous to an eggshell. Existing work has demonstrated that these spinodal metamaterials exhibit near-optimal stiffness-to-density, have highly customizable directional properties (anisotropy), and high recoverability. However, their performance under dynamic loading—pertinent to their potential application to engineering problems—remains unexplored.

this work, we computationally and experimentally demonstrate how curvature in shellbased spinodal metamaterials determines their ratedependent mechanical responses. To do this, we model the phase separation process and fabricate spinodal structures using two-photon lithography—a highresolution, three-dimensional printing process—and then perform nanomechanical dynamic experiments with high speed in situ microscopy to observe deformation modes and behavior. We demonstrate ratestiffening in spinodal metamaterials that surpasses (by ~50%) the expected rate-stiffening of the constituent material. Through computational studies of both spinodal and reference periodic architectures, we reveal that shell-based spinodal metamaterials exhibit a wide range of localization responses due to their double curvature and aperiodicity relative to periodic architectures. These findings offer a pathway for the design of energy-absorbing metamaterials with enhanced and programmable rate sensitivity and suggest spinodal architectures as a promising route toward scalable, application-ready dynamic materials.

Dynamic Behavior of Architected Materials

Shell-Based Architectures Periodic Beam-Based Architectures

Dynamic Nanomechanical Experiments Fabrication Experiment



▲ Figure 1: Dynamic behavior of Shell-based architected materials.

Atomic Layer Etching of Overlying Epitaxial Graphene on Graphene Buffer Layer for a Scalable Remote Epitaxy Template

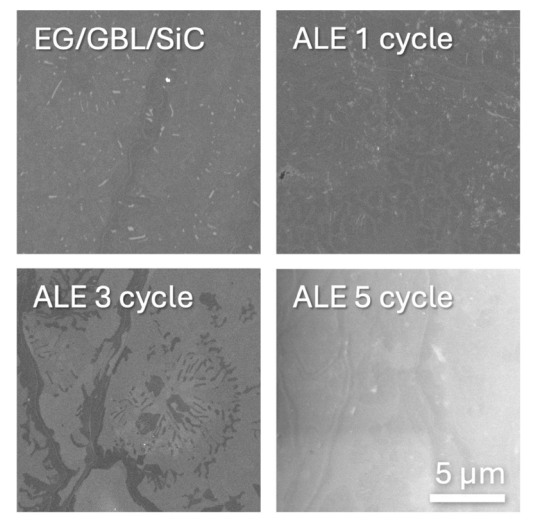
J. Lee, J. Feng, J. Kim, S. H. Cho, S. Lee, J. Kim, J. Kim

Freestanding single-crystal membranes hold transformative potential for next-generation electronic and optoelectronic devices due to their ultrathin form factor, flexibility, and integra-tion versatility. Among fabrication techniques, remote epitaxy has emerged as a powerful route to produce transferable single-crystal membranes by leveraging long-range electrostatic interactions through atomically thin two-dimensional (2D) interlayers. Graphene buffer layers (GBLs) formed on silicon carbide (SiC) substrates via high-temperature graphitization have gained attention as ideal 2D templates. However, conventional graphitization unavoidably gen-erates overlying epitaxial graphene (EG) layers on top of the GBL, which must be selectively removed to maximize remote interaction and substrate pattern transfer. Previous EG removal methods—such as mechanical exfoliation or chemical etching-often degrade the underlying GBL, hindering remote epitaxy performance.

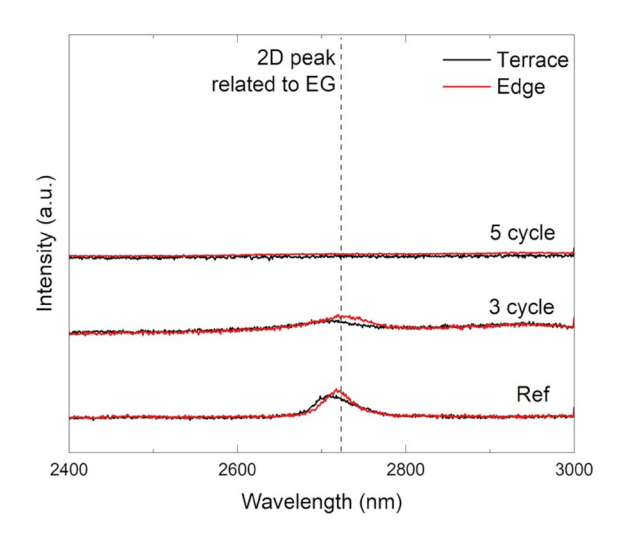
In this work, we introduce a selective atomic layer etching (ALE) technique to remove EG while

preserving the integrity of the underlying GBL. Our approach exploits the differential bonding strengths: EG is weakly bound to the sp²-hybridized GBL, whereas the GBL is partially covalently bonded to the SiC substrate. By tailoring etching conditions to this interfacial energy contrast, we achieve layer-by-layer removal of EG without damaging the GBL. Surface and structural analyses confirm the preservation of a pristine, atomically flat GBL surface—essential for enhancing remote substrate interaction and enabling high-quality remote epitaxi-al growth.

This ALE-based approach provides a scalable route to prepare high-quality GBL templates for remote epitaxy. Building on this foundation, we aim to demonstrate the growth and exfoli-ation of freestanding GaN membranes via remote epitaxy in future work. Our results lay the groundwork for defect-free GBL engineering and highlight a critical step toward realizing wafer-scale manufacturing of freestanding semiconductor membranes.



▲ Figure 1: Scanning electron microscopy (SEM) top-view for before/after of atomic layer etching of EG on GBL/SiC substrate – EG removal in SEM with ALE 5 cycle.



▲ Figure 2: Raman analysis for ALE of EG on GBL/SiC substrate – 2D peak disappearance in Raman with ALE 5 cycle.

FURTHER READING

S. Lee, J. Kim, B.-I. Park, H. I. Kim, C. Lim, E. Lee, J. Y. Yang, J. Choi, Y. J. Hong, C. S. Chang, H. S. Kum, J. Kim, K. Lee, H. Kim, and G.-C. Yi, "GaN Remote Epitaxy on a Pristine Graphene Buffer Layer via Controlled Graphitization of SiC," Appl. Phys. Letts. DOI: 10.1063/5.0235653

Fluctuations in Superconducting Nanowires

E. Batson, A. Jacquillat, A. Simon, F. Incalza, R. Foster, K. K. Berggren Sponsorship: NSF GRFP Grant No. 2141064, NSF CQN Grant No. EEC1941583

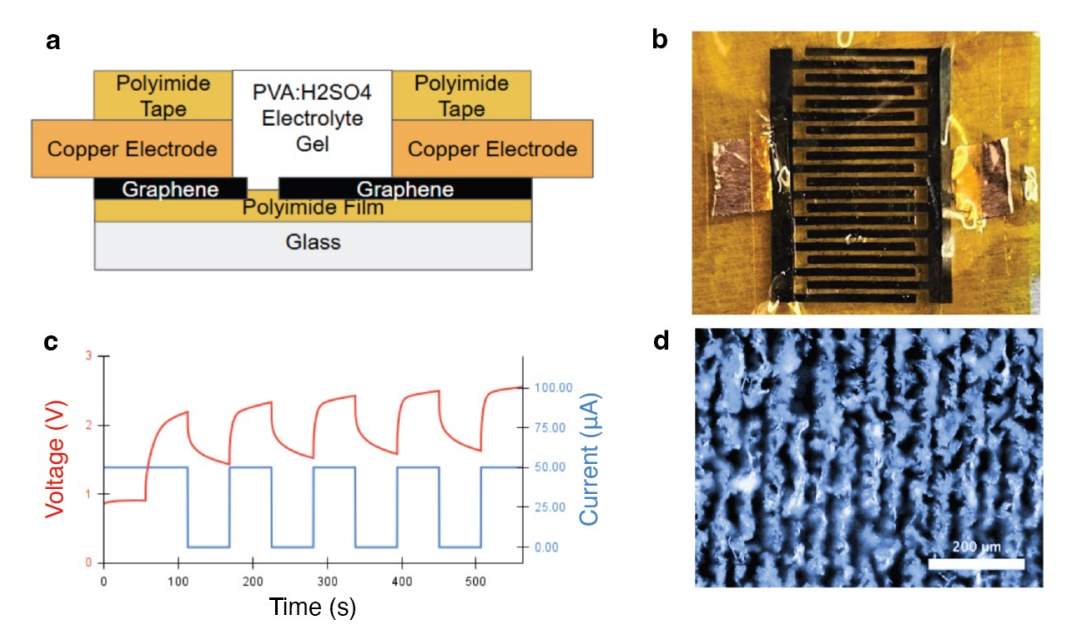
Superconducting nanowire single photon detectors (SNSPDs) provide sensitive, highly efficient detection out into the mid-infrared, suitable for low-signal applications like exoplanet search, quantum networking, and biomedical imaging. However, the physics of these devices is complex, and the detection mechanism is not well understood, which makes it difficult to predict the success of new material platforms or develop designs that decrease dark counts while preserving high detection efficiency. In this work, we study dark fluctuations in niobium nitride nanowires of various lengths and widths and compare the fluctuation rates to various models of the underlying mechanism. We evaluate whether it is more appropriate to attribute these fluctuations to one-dimensional phase slips or two-dimensional vortices activated by either flux entry or a topological phase transition. We also consider the role of external noise sources such as blackbody radiation or current source noise.

Laser-induced Graphene Supercapacitors

A. Arroyo, C. Lowe, F. Kelley, E. Szczepaniak, K. Muhammad, P. Jastrzebska-Perfect Sponsorship: MIT EECS, 6.2540 class

Supercapacitors, which demonstrate power densities comparable to those of batteries while providing fast charging and discharging capabilities, have gained favor in energy storage applications requiring fast power transfer, like electric vehicles or power grids. To achieve high capacitances, porous electrodes, which maximize electrolyte-electrode interaction, are utilized. For supercapacitors to be generally applied, scalable, repeatable, and cost-effective methods for fabricating such electrodes are required. Here, we demonstrate a meth-

od for manufacturing supercapacitors based on high surface area laser-induced graphene electrodes. We use a laser-based fabrication process that enables tuning of the electrode conductivity through empirically-determined power-conductivity relationships. Through optimization of laser power level, substrate choice, and details of the optical setup, we achieve devices with a specific capacitance of 0.7 mF/cm². This approach provides an accessible and scalable method for manufacturing graphene supercapacitors.



▲ Figure 1: a) Illustration of the designed supercapacitor's cross section. b) Image of a working supercapacitor. c) Charge and discharge curves of a working capacitor when applying pulses of current. d) Microscope image of laser-induced graphene surface.

Hydrogen Gas Detection with MoS₂-based Chemical Sensing Platform

C.-H. Liu, J. Zhu, C. Lopez Angeles, H. Feng, T. Swagger, J. Kong, T. Palacios Sponsorship: Palacios Lab

Hydrogen is a promising candidate as a clean energy carrier for its high energy density, clean combustion byproduct, and versatile end use. However, its explosive nature calls for the need for rapid and accurate detection. Two dimensional (2D) materials are ideal candidates for such application thanks to their naturally surface-sensitive properties and large surface-to-volume ratio, providing high sensitivity towards the target gas.

In this work, we developed a field effect transistor-based sensor that employs functionalized molybdenum disulfide (MoS₂) as the channel material.

Threshold voltage shift under hydrogen and surface functionalization of the ${\rm MoS}_2$ to further enhance sensitivity are demonstrated. Thanks to the 8" low-temperature (< 400 °C) synthesis of high-quality ${\rm MoS}_2$, the ${\rm MoS}_2$ sensors can be further integrated into a robust sensing array in which each device can be functionalized with different sensing materials and combinations. Future work involves the development of a high-speed readout electronic circuit with a total processing speed below 1 second, establishing an integrated system that can perform rapid measurement, analysis, and real-time chemical recognition.

FURTHER READING

[•] J. Zhu, J. Park, S. A. Vitale, et al., "Low Thermal Budget Synthesis of Monolayer Molybdenum Disulfide for Silicon Back-end-of-line Integration on 200 mm Platform," Nat. Nanotechnol. 18, 456-463 (2023).

Signatures of Chiral Superconductivity in Rhombohedral Graphene

T. Han, Z. Lu, Y. Yao, L. Shi, J. Yang, J. Seo, S. Ye, Z Wu, M Zhou, H. Liu, G. Shi, Z. Hua, K. Watanabe, T. Taniguchi, P. Xiong, L. Fu, L. Ju

Sponsorship: DOE (DE-SC0025325), NSF (DMR-2225925), NSF (DMR-1231319)

Chiral superconductors are unconventional superconducting states that break time reversal symmetry spontaneously and typically feature Cooper pairing at non-zero angular momentum. Such states may host Majorana fermions and provide an important platform for topological physics research and faulttolerant quantum computing. Despite intensive search and prolonged studies of several candidate systems, chiral superconductivity has remained elusive so far. Here we report the discovery of robust unconventional superconductivity in rhombohedral tetra-layer graphene. We observed two superconducting states in the gate-induced flat conduction bands with Tc up to 300 mK and charge density no as low as 2.4 x 10^{11} cm^{-2} in three different devices, where electrons reside close to a proximate WSe, layer, far away from WSe, and in the absence of WSe, respectively. Spontaneous time-reversal-symmetry-breaking (TRSB) due to electron's orbital motion is found,

and several observations indicate the chiral nature of these superconducting states, including: 1. In the superconducting state, R_{xx} shows fluctuations at zero magnetic field and magnetic hysteresis in varying outof-plane magnetic field B_⊥, which are absent from all other superconductors; 2. one superconducting state develops within a spin- and valley-polarized quartermetal phase, and is robust against the neighboring spin-valley-polarized quarter-metal state under B1; 3. the normal states show anomalous Hall signals at zero magnetic field and magnetic hysteresis. We also observed a critical B₊> 0.9 T, higher than any graphene superconductivity reported so far and indicates a strong-coupling superconductivity close to the BCS-BEC (Bardeen-Cooper-Schrieffer - Bose-Einstein condensate) crossover. Our observations establish a pure carbon material for the study of topological superconductivity, and pave the way to explore Majorana modes and topological quantum computing.

Domain-controlled Growth of Two-dimensional Tin Selenide

Y. Zhu, T. Zhang, N. Mao, J. Wang, J. Kong Sponsorship: DOE Basic Energy Sciences under Award DE-SC0020042

Two-dimensional (2D) van der Waals (vdW) layered materials have become a hot research topic in the fields of condensed matter physics and materials science due to their unique low-dimensional crystal structures and physical properties. 2D tin selenide (SnSe) is a vdW layered material with a strong spontaneous ferroelectric polarization and second-order nonlinear optical response, whose ferroelectric properties and second-order nonlinear optical characteristics are enhanced in its ferroelectric-stacking (FE-stacking) phase, a metastable phase at room temperature. Large-sized ultrathin 2D SnSe crystals have been synthesized via a physical vapor deposition (PVD) approach, but the control of FE-stacking and domain distribution remains a challenge.

In this work, the domain control of 2D SnSe

is preliminarily achieved by growth condition modulation and substrate engineering. A PVD growth recipe for 2D SnSe is optimized, that yields the most FE-stacking phase crystals, and a dependence of domain distribution density on substrate condition is identified. A pre-annealing treatment of the mica substrate in air not only improves the 2D SnSe samples' size and distribution on substrate, but also promotes the synthesis of samples with dense FE-stacking domains. The next step is to apply an electric field to the 2D SnSe material during PVD growth, which modulates the energy of the FE-stacking metastable phase compared to the stable phase, providing a possible pathway to achieve the controlled growth of FE-stacking 2D SnSe.

Molecular Probe Adsorption as a Technique to Elucidate Corona Phase Molecular Recognition (CoPhMoRe) through Structure Property Relationships

G. Sánchez-Velázquez, D. T. Khong, M. Park, X. Jin, X. Gong, Z. Yuan, M. C.-Y. Ang, M. S. Strano Sponsorships: NSF Graduate Research Fellowship Program, Singapore-MIT Alliance for Research & Technology (SMART)

The nanoparticle corona—a molecular layer adsorbed on nanoparticle surfaces—is critical in controlling molecular interactions for applications in catalysis, separations, and sensing technologies like Corona Phase Molecular Recognition (CoPhMoRe). While tailoring the corona has enabled detection of diverse analytes, quantitatively characterizing it remains challenging. Here, we advance Molecular Probe Adsorption (MPA) to address this issue. MPA employs a fluorescent probe quenched upon adsorption to quantify the solvent-exposed surface area via adsorption isotherms. We use MPA to elucidate recognition mechanisms in various corona phases and expand the library by characterizing new CoPhMoRe constructs, enabling comprehensive comparative analyses. We further develop structureproperty relationships linking MPA area to adsorption parameters. Additionally, we investigate how polymer

stiffness, characterized by persistence length, influences corona formation on single-walled carbon nanotubes (SWCNTs). Contrary to the assumption that stiffer polymers enhance adsorption efficiency, our results indicate that more flexible polymers achieve greater surface coverage, offering new insights for optimizing polymer-based corona phases. We also tackle the inverse problem of predicting analyte binding affinities by integrating MPA with molecular dynamics simulations and thermodynamic modeling, demonstrating that computational CoPhMoRe screening is feasible. This integration paves the way for rational sensor design without extensive experimental screening. Our findings highlight MPA's utility in advancing nanomaterial-based sensing technologies through quantitative corona characterization and provide a framework for the rational design of selective nanosensors.

Optimizing Contact Resistance of GaN p-FET Devices for CMOS Applications

J. Park, J. Niroula, J. Hsia, T. Palacios Sponsorship: Lincoln Laboratory

Gallium nitride (GaN) transistors have a much higher break-down voltage, switching frequency, and maximum operating temperature than their silicon (Si) counterparts. However, because GaN transistors are largely limited in performance by the Si gate driver and other ancillary chips, GaN transistors need to be integrated with GaN driver chips to fully realize their energy efficiency in power electronics applications and high-temperature environments. The most energy-efficient architecture for integrated circuits and drivers is complementary metal oxide semiconductor (CMOS) circuitry, which requires n-type field effect transistors (n-FETs) and p-type field effect transistors (p-FETs). While GaN n-FETs have been widely demonstrated,

GaN p-FETs are traditionally difficult to fabricate with good performance and integrate into CMOS circuits.

A primary source behind the current density limitations of a GaN p-FET device is the high contact resistance. Prior work in the Palacios group at the Massachusetts Institute of Technology (MIT) has shown record GaN p-FET performance; however, these devices are still largely limited by the contacts. In this project, we will explore different deposition methods and metals for achieving low contact resistance on GaN p-FETs. Ultimately, this work on improving contact resistance of GaN p-FETs will enable a fully integrated GaN-based CMOS platform.

Optical Detection of Proximity Effect Between WSe_2 and Multiferroic Helimagnet Nil_2

M. Shankar, Q. Song, R. Comin Sponsorship: National Science Foundation (DMR-2405560), Peskoff Physics Fellowship

Magnetic proximity effects have been widely investigated in layered heterostructures to imprint the properties of one material to be detected on the other. In many cases, studying the proximity effect of a magnetic material on another material can reveal properties about the former that are not otherwise straightforward to detect. NiI, is a type-II multiferroic that exhibits a simultaneous ferroelectric and non-collinear helimagnetic transition at T_N = 59.5 K, where the spin helix has propagation vector q = (0.138, 0, 1.457) RLU. It exhibits strong optical linear dichroism related to the ferroelectric transition, but direct optical detection methods of the chirality of the spin helix, which is coupled to the direction of the ferroelectric polarization, have remained elusive. Monolayer WSe, is effective for studying a variety of optical phenomena due to its direct bandgap and spin-valley locking, namely exhibiting very strong photoluminescence; thus, putting it in

proximity to NiI, enables additional optical techniques to interpret properties of the latter. In this study, we report circular dichroism in the photoluminescence of a monolayer WSe, and NiI, heterostructure that switches sign upon reversing the electric polarization of the NiI₂. We attribute the dichroism to the type-II band alignment of the semiconductor-insulator interface and the spin-polarized momentum splitting of the Nil, bands along the direction of the spin helix. In addition, we compare the reflective circular dichroism of the heterostructure to the reflective magnetic circular dichroism (RMCD) of the isolated WSe, monolayer to estimate the magnitude of the magnetic proximity effect. These results demonstrate a novel optical detection method of magnetic chirality switching in an odd-parity multiferroic, expanding the methods to distinguish symmetry breaking phenomena in unconventional magnetic systems.

On-site Growth of Perovskite Nanocrystal Arrays for Integrated Nanodevices

P. Jastrzebska-Perfect, W. Zhu, M. Saravanapavanantham, Z. Li, S. O. Spector, R. Brenes, P. F. Satterthwaite, R. Ram, F. Niroui Sponsorship: NSF

Known for their superior optoelectronic properties, halide perovskites have been utilized to realize applications such as solar cells, light-emitting diodes, memristors, and single photon-sources. However, integrating halide perovskites in nanoscale devices has remained challenging, given the chemical incompatibilities of these materials with conventional lithographic processing techniques. Here, we introduce a bottom-up approach for precise and scalable formation of perovskite nanocrystals and their integration into functional nanodevices. Our approach uses topographical templates with asymmetric surface wettability to guide the site-selective growth of the perovskite nanocrystals. With this platform, we demonstrate arrays of CsPbBr₂ nanocrystals with tunable dimensions down to < 50 nm and placement accuracy < 50 nm. We further apply our approach to develop nanoscale light-emitting diodes (nanoLEDs), highlighting the potential this platform offers for enabling on-chip perovskite nanodevices.

Probing Operational Degradation Mechanism on Cd-free Red and Blue QD-quantum dot LEDs

R. Zhang, V. Bulović Sponsorship: Samsung Electronics, MIT 2024 Mathworks Fellowship

With a variety of emerging display products like AR/VR, smart watch, etc., high quality display materials are required. Cadmium-free colloidal quantum dots have been reported as promising candidates in quantum dot light-emitting diodes (QD-LEDs) due to their tunable optical properties, quantum confinement effects and scale-up capability. However, comparing to the high operational lifetime of red and green QD-LEDs counterparts, the blue QD-LEDs offer a much lower operation lifetime. In this work, we probe the operation degradation mechanisms on both InP/ZnSe/ZnS (red) and ZnSe(Te)/ZnSe/ZnS (blue) QD-LEDs from a perspective of nanoscale device morphology and interlayer elemental tracing. A coarsening and thinning phenomenon is observed in both quantum dots and Mg-doped

zinc oxide nanoparticles (ZnMgO NPs) layers after red QD-LED LT-50 aging and blue QD-LED LT-70 aging. An extra oxygen peak shows up in the InP/ZnSe QD layer after biasing the device, where the compositional oxygen level enhances at the Al electrode / ZnMgO NPs junction. Additionally, our findings indicate that long-time high-dose electron beam irradiation contributes to the coarsening of the ZnMgO NP layer, and the presence of hydrogen significantly accelerates the coarsening process under electron beam exposure. This study reveals the morphological thinning and particle coarsening in the electron transporting layer (ETL) and active layer after diode aging, establishing a framework for understanding QD-LED degradation mechanisms during operation.

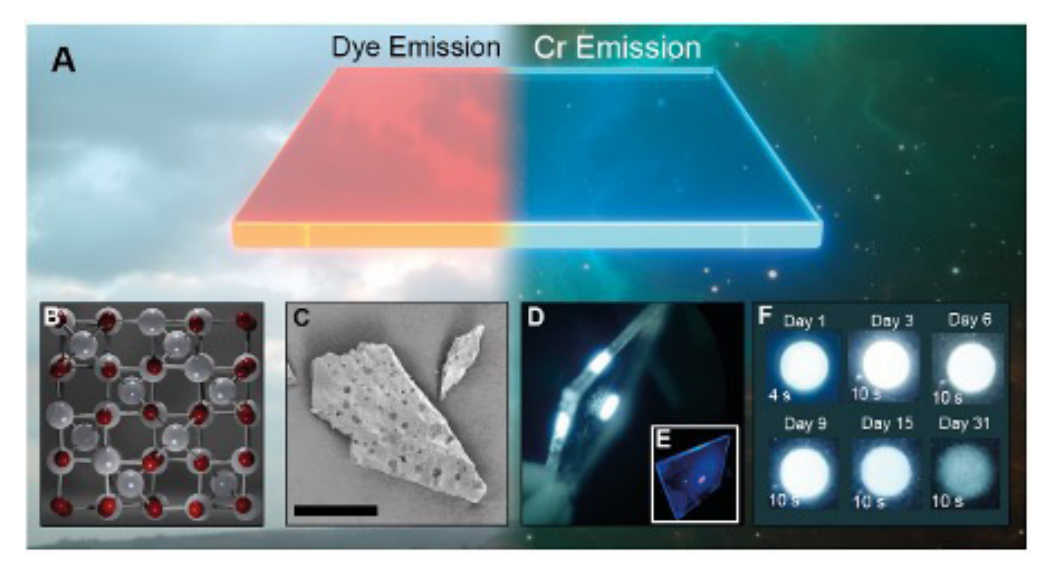
Solid State Solar Energy Storage from Persistently Luminescent Solar Concentrators

T. K. Baikie

Sponsorship: Schmidt Science Fellowship, Lindemann Trust Fellowship

The remarkable reduction in the levelized cost of energy (LCOE) for solar power has meant that photovoltaics have become increasingly competitive with fossil fuels, yet challenges remain in achieving the widespread adoption necessary to meet global climate targets. One of the primary barriers is the inherent variability of photovoltaic (PV) output, driven by short-term fluctuations in environmental conditions, which undermine the output stability and predictability re-

quired in energy markets that rely on spot pricing. We propose an alternative approach to stabilize solar output by artificially delaying the photon flux incident on conventional solar cells using persistently luminescent chromophores within solar concentrator devices. This approach aims to smooth the output power with minimal impact on overall efficiency, providing a pathway to enhance the economic viability and reliability of solar energy in grid-scale applications.



▲ Figure 1: **A** – Cartoon depiction of the two emission modes. Dye emission under bright conditions and long lifetime emission from Cr. **B** – Structure of long-lived emissive crystal determined from XRD. A single unit cell of $Zn_3GaGe_2O_8$, where Zn, Ga and Ga are shown in grey, Ga is shown in red. Thermal parameters were refined by element and are not shown to scale. **C** - Indicative SEM image of particles. Scale bar is X um. **D** – 10 by 10 cm PLSC device photographed 1 hour after illumination in dark conditions in the IR with **E** inset a photo at visible wavelengths under blue illumination. **F** Active area photographed in the IR for a period of a month after illumination with different integration times inset.

Electrical Double Layer Force Enabled Wafer-scale Transfer of van der Waals Materials

X. Zheng, J. Wang, J. Jiang, T. Zhang, J. Zhu, T. Dang, P. Wu, A. Lu, D. Chen, T. H. Yang, X. Zhang, K. Zhang, K. Y. Ma, Z. Wang, Y. Hsieh, V. Bulović, T. Palacios, J. Kong

Sponsorship: US Army Research Office, Air Force Office of Scientific Research (AFOSR) Multi-University Research Initiative

The transfer and integration of van der Waals (vdW) materials to target substrates is critical to their applications in high-end electronics, optics, moiré electronics, etc. The transfer step typically requires the use of either chemical etchants, electrochemical bubbling, or mechanical strain to detach vdW materials from growth substrate. However, these approaches often have issues regarding contamination, degradation of vdW materials or damage of growth substrates (adding significant cost to the manufacturing process, especially for single crystalline substrates). In this work, we present an electrical double layer (EDL) force enabled transfer method that is etching-free, fast, highly reliable and widely applicable to various types of substrates (e.g., oxide, nitride, etc.) and materials (e.g., carbon nanotube, MoS₂, h-BN, etc.). The unique strategy is to leverage the negative zeta potential of both the substrate and the

vdW material in concentrated ammonia solution. With the formation of the EDL, the vdW material is repelled from the substrate by the strong EDL repulsion force. The as-transferred vdW materials show minimized wrinkles, cracks, contaminations, and other transfer-induced defects. The $\rm MoS_2$ field effect transistors fabricated with EDL transfer show 100% yield, near-zero hysteresis (7 mV) and near-ideal subthreshold swing (65.9 mV/dec), evidencing an ultra-clean interface and minimized damage. The combination of EDL transfer and bismuth contact further enables an ultra-high on-current of 1.3 mA/ μ m. This EDL transfer approach offers a facile and manufacturing-viable solution for vdW material integration, which will significantly advance the future development of atomically thin electronics.

88